Structure of avalanches and breakdown of simple scaling in the Abelian sandpile model in one dimension

Agha Afsar Ali and Deepak Dhar
Theoretical Physics Group, Tata Institute of Fundamental Research, Homi Bhabha Road, Bombay 400 005, India
(Received 7 June 1995)

We study the Abelian sandpile model on decorated one-dimensional chains. We show that there are two types of avalanches, and determine the effects of finite, though large, system size L on the asymptotic form of distributions of avalanche sizes, and show that these differ qualitatively from the behavior on a simple linear chain. For large L, we find that the probability distribution of the total number of topplings s is not described by a simple finite-size scaling form, but by a linear combination of two simple scaling forms: $\mathrm{Prob}_L(s) = \frac{1}{L} f_1(\frac{s}{L}) + \frac{1}{L^2} f_2(\frac{s}{L^2})$, where f_1 and f_2 are nonuniversal scaling functions of one argument.

PACS number(s): 05.40.+j

I. INTRODUCTION

The sandpile model is a simple cellular automaton model, introduced by Bak, Tang, and Wiesenfeld in 1987 to illustrate the phenomena of self-organized criticality (SOC) [1]. Since then several sandpilelike automata have been studied [2–6]. Similar cellular automata have been proposed as models of other self-organizing systems, e.g., earthquakes [7,8], forest fires [9], neural networks [10], and potential energy fluctuations in liquid water [11]. However, the precise conditions under which the steady state of a driven system shows critical (long-range) correlations are not well understood, in particular, in nonconservative systems [12–14]. In systems with conservation laws, for example, in sandpile models with local conservation of sand, it is easily shown that the moments of distribution of avalanche sizes diverge as powers of the system size [15–18]. This, however, does not necessarily imply power law tail in the distribution of avalanche sizes (see, for example, [19]), as these can be accounted for by rare large events.

As we still do not understand what conditions are necessary, or sufficient, for the onset of criticality in driven dissipative systems, most studies of SOC depend upon numerical simulations for evidence of criticality. To incorporate the effect of finite-size cutoffs, one usually fits numerical data to a finite-size scaling form in which the critical exponents of the infinite system appear as parameters. However, on the basis of extensive numerical studies of several one-dimensional sandpile automata, Kadanoff *et al.* [5] and Chhabra *et al.* [20] have argued that because of the presence of more than one characteristic length scale in many of these models, simple finite-size scaling theory does not correctly describe the distribution of avalanche sizes. These authors found that a more general "multifractal" scaling form was necessary to get satisfactory fits to their Monte Carlo data.

As the finite-size scaling assumption based on a single scaling form is widely used in the numerical studies of SOC, it seems desirable to test it in analytically tractable models. This we do in this paper for a class of one-dimensional sandpile models, which are special cases of the general Abelian sandpile model (ASM). The ASM is perhaps the simplest of the models showing self-organized criticality [17]. It is of special interest because of its analytical tractability, which arises mainly from the Abelian property. Several interesting results for the critical state and the critical exponents are known [21–24]. The model has been solved exactly in one dimension [1,25], on the Bethe lattice [26], and in the mean field limit [27]. The ASM with a preferred direction of particle transfer turns out to be equivalent to the voter model, and all the critical exponents can be determined in all dimensions [28]. Recently the structure of the Abelian group has been determined in terms of the toppling matrix [29].

We consider the ASM on one-dimensional chains formed by joining a single type of unit cells (see Fig. 1). Such decorated chains are the simplest generalization of the linear chain. We have studied two cases in detail. Case A is a chain of alternating double and single bonds. Case B is a chain of diamonds joined together by single bonds. We solve analytically the ASM on these graphs in the limit of large system size L, and find that the avalanche distribution function shows a nontrivial scaling behavior (a brief account of this work has appeared earlier [30]). The properties of the ASM on these chains are very different from those on the simple linear chain, which has been studied earlier by Bak *et al.* [31], and in more detail recently by Ruelle and Sen [25]. In fact, the behavior of the ASM on a simple linear chain is not

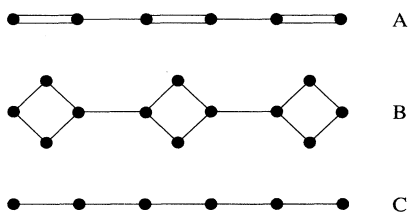

FIG. 1. The one-dimensional chains formed by joining (A) doublets, (B) diamonds, (C) single sites.

 ©1995 The American Physical Society

typical of one-dimensional ASM's.

In case A (and also in case B), we find that there are two types of avalanches type I and type II. Type I avalanches spread a distance of order L on one side of the point where a particle has been added and a distance of order 1 on the other side. As a result the number of toppling at any site is of order 1, and the total number of toppling in an avalanche scales as L. In contrast, type II avalanches spread a distance of order L on both sides, the number of topplings on a site scales as L, and the total number of topplings in an avalanche scales as L^2.

We find that, for large L, the distribution functions of duration t of an avalanche, and of the number of distinct sites toppled s_d in an avalanche, do have a simple scaling form in our model. However, the distribution functions of the total number of topplings s, and of the maximum number of topplings n_c at any one site, do *not* have a simple scaling form, but a more complicated linear combination of two simple scaling forms (LC2SSF)

$$\mathrm{Prob}_L(X) = L^{-\beta_1} f_1(X L^{-\nu_1}) + L^{-\beta_2} f_2(X L^{-\nu_2}) \quad \text{for large } L\ , \qquad (1)$$

where X is a random variable measuring the "size" of the avalanche, and β_1, ν_1 and β_2 and ν_2 are critical exponents. For $X = n_c$, $\beta_1 = \nu_1 = 0$ and $\beta_2 = \nu_2 = 1$. For $X = s$, $\beta_1 = \nu_1 = 1$ and $\beta_2 = \nu_2 = 2$. The scaling functions f_1 and f_2 are also different for different X's. We also find that this behavior is quite robust and does not depend on the choice of the unit cell, but in general the function f_1 and f_2 are not universal. We expect similar behavior in the ASM on other effectively one-dimensional graphs, in which the system has large extent in only one dimension and only finite extent in transverse dimensions (for example, a long cylinder).

The plan of this paper is as follows. In Sec. II, we define precisely the cases A, B, and C dealt with in this paper. The analysis of case A and B is quite similar. We shall confine ourselves mainly to case A in this paper, and only briefly summarize results obtained by us for case B towards the end. Case C is already well studied and is included here only for comparison. In Sec. III, we characterize the recurrent configurations of the model for case A. We find that the total number of recurrent configurations grows exponentially with the size of the system. As a result, the entropy per site in the SOC state is nonzero even as $L \to \infty$. We determine the distribution of heights in the critical steady state of the model and find that it shows nontrivial dependence on the distance from the boundary. Sections IV–VII are devoted to the study of the propagation of avalanches in case A. In Sec. IV, we use the decomposition of an avalanche into waves of topplings, introduced by Ivashkevich *et al.* [32], which greatly simplified the analysis of the avalanches. In the analysis of the waves of topplings, we are led to introduce a transfer operator, which transfers a particle from a unit cell to its neighboring unit cell without relaxing the configuration. The relaxation rules are then recast as relaxation rules for this operator. In Sec. V, we discuss the propagation of avalanche front using the properties of the transfer operator for the type I and the type II avalanches on the doublet chain. In Sec. VI, we calculate the probability distributions of the linear extent of avalanche s_d, the duration of avalanche t, and the total number of topplings s. In Sec. VII, we analyze the probability distribution of avalanche size in terms of multifractals, and support our analysis with numerical simulation. In Sec. VIII, we briefly outline how the analysis of Secs. IV–VII can be extended to diamond chain (case B), and its differences from case A. Section IX contains a summary of our results, and a discussion of possible extension to ASM's on long cylinders, which seems to be a promising way to study the ASM in two dimensions.

II. DEFINITION OF THE MODEL

The model is defined as follows. A site on the chain is denoted by a pair of indices (i, j), where $i = 1$ to L labels the unit cell, and j numbers a site within the unit cell. In case A, j ranges from 1 to 2. In case B, j ranges from 1 to 4, with sites within a unit cell labeled in a clockwise direction starting from the left site. At each site (i, j) there is an integer height variable h_{ij}. The dynamics of sandpile involves the following two types of steps.

(i) Addition of particles: A particle is added at a randomly selected site by increasing the height at that site by 1.

(ii) Toppling: If the height h_{ij} is greater than a preassigned threshold height h^c_{ij} at that site, it topples. Its height decreases by h^c_{ij}, and one particle is transferred along each bond connecting it to its neighbors.

We choose h^c_{ij} to be independent of i and equal to the coordination number of site of type j. For example $h^c_{ij} = 3$, for all the sites in case A. In case B, $h^c_{ij} = 2$, for $j = 2$ and 4, and $h^c_{ij} = 3$, for $j = 1$ and 3. Clearly, the topplings conserve the number of particles in bulk but each toppling at a boundary site causes a loss of one particle from the system. The process of toppling continues until there are no unstable sites. The sequence of topplings caused by addition of one particle is called an avalanche. A new particle is added after the avalanche has stopped.

III. CHARACTERIZING THE RECURRENT CONFIGURATIONS

The critical steady state is easy to characterize using the general theory of ASM's [17]. The configurations that occur in the steady state with nonzero probability are called recurrent configurations. These configurations occur with equal probability. The set of recurrent configurations may be characterized by the burning algorithm ([17], see also [33]). In this algorithm, we start with a configuration in which all the sites are unburnt. A site is "burnt" if its height is greater than the number of bonds joining it to its unburnt neighbors. The configuration which can be fully burnt is called an "allowed" configu-

ration. It has been shown in Ref. [17] that the allowed configurations form a closed set under the dynamics of the ASM. We will summarize the proof in brief here. Let us assume the contrary. Then there is an allowed configuration C, such that, after the toppling of a site i, it becomes C' which is not allowed. Let F be the set of sites which cannot be burnt in C'. From the rule of the ASM it is obvious that in configuration C, the set of sites which is obtained by deleting site i from F cannot be burnt. This contradicts our assumption that C is allowed. Hence the set of allowed configurations is closed. A stable allowed configuration is clearly a recurrent configuration. It was later shown by Speer [33] that all the recurrent configurations are allowed.

In the burning algorithm, the sites can be burnt in any order, and the final result is independent of the order in which the sites are burnt. The first site which can be burnt is clearly a boundary site. We choose the convention that the burning starts from the left boundary and continues rightward as long as possible. The unit cell where the rightward burning stops will be called the break point (BP). Afterwards, the burning is allowed to proceed leftwards from the right boundary.

Let us now consider case A. It is easy to see using the burning algorithm that the allowed values of (h_{i1}, h_{i2}) in a recurrent configuration for i on the left of the BP are $(3,3)$ and $(3,2)$. For i on the right of the BP these are $(3,3)$ and $(2,3)$, and at the BP these are $(2,3)$, $(3,1)$, and $(1,3)$. In the following, we shall call the doublet $(3,3)$ as type A, $(3,2)$ as type B_1, and $(2,3)$ as type B_2. The doublets $(3,1)$ and $(1,3)$ shall be called of type C_1 and C_2, respectively. Thus a configuration of sandpile is denoted by a string of these symbols. For example, $AAB_1AC_1B_2AB_2$ represents a configuration for $L = 8$ chain in which the first two doublets are of type A, the third is of type B_1, etc. It is easy to see that the formal sum over all the strings corresponding to the recurrent configurations is given by

$$Z = (A + B_1)^L + \sum_{r=1}^{L} (A + B_1)^{r-1} \times (B_2 + C_1 + C_2)(A + B_2)^{L-r} \ . \qquad (2)$$

The total number of recurrent configurations is obtained by substituting 1 for each of the formal symbols in the above expression. Thus the number of recurrent configurations for a chain of size L is $(1 + \frac{3}{2}L)2^L$. Consequently, the entropy per site (defined as the logarithm of the total number of recurrent configurations divided by the number of sites) is equal to $\ln(2)/2$ in the large L limit. For the simple linear chain, the entropy per site in the SOC state is zero. This fact is responsible for its nongeneric behavior.

To the left (right) of the BP, the left (right) site of a doublet always has height 3, and the right (left) site of a doublet has height 2 and 3 with probability $\frac{1}{2}$ for each. The BP can occur at any of the L doublets with equal probability. Averaging over the position of the BP, this implies that the probabilities of the left site of the ith doublet having height 2 and 3 are $i/(2L)$ and $1 - i/(2L)$, respectively [we assume that L is large, so that we need not distinguish between L and $(L + 1)$, etc.]. Similarly the probabilities of the right site of a doublet having height 2 and 3 are $\frac{1}{2}(1 - i/L)$ and $\frac{1}{2}(1 + i/L)$, respectively. Thus the average height profile in the SOC state varies linearly with i in case A, and the SOC state is *not translationally invariant even far away from the boundaries.* This feature is not present in case C.

IV. TRANSFER OPERATOR

To analyze the structure of avalanches, it is useful to define a decomposition of avalanches into subavalanches. One such decomposition was defined in Ref. [34], in terms of subavalanches called "inverse avalanches." It uses the "untoppling" process, which is the inverse of the toppling process. Later Ivashkevich *et al.* showed that the same decomposition can be realized more simply, without introducing untopplings, in terms of "waves of topplings" [32]. From the Abelian property of the ASM, we can topple unstable sites in any order; the resulting final configuration is the same. Thus we may choose the following order: Topple the source site once and let all other sites topple until they are stable. This sequence of topplings is called the first wave of topplings. After this, if the source site is still unstable, it is toppled once more and the rest of the sites are allowed to relax. This constitutes the second wave of topplings. This process continues until the whole configuration becomes stable.

It is easy to see that the waves of topplings propagate in exactly the same way as the burning front in the burning algorithm. Thus a unit cell which cannot be fully burnt from the left (right) side stops a wave propagating towards it from the left (right). We refer to such configurations as left (right) stoppers. However, the stopper is itself modified in the process of stopping a wave, so that the next wave may cross it. It thus stops a wave of topplings coming towards it (if from a favorable direction), but cannot stop an avalanche which is a sequence of waves. It only slows down the spreading of an avalanche.

Let us denote the unstable doublet obtained by adding a particle at the left and the right side of the doublet X_i by ${}^*X_i$ and X_i^*, respectively. In calculating the propagation of a wave of topplings, it is convenient to define an operator t which transfers a particle from the right site of a doublet to the left site of the adjacent doublet to the right. Thus $X_1 X_2 \ldots X_n \, t \, X_{n+1} \ldots$ is the (possibly unstable) configuration resulting from the configuration $X_1 X_2 \ldots X_n X_{n+1} \ldots$, by transferring a particle from the right site of the nth doublet X_n to the the left site of X_{n+1}. We define t^{-1} as the inverse of t. Then $X_1 X_2 \ldots X_n \, t^{-1} \, X_{n+1} \ldots$ is the configuration obtained, if one transfers a particle from the left site of a doublet $X_{n+1}$to the right site of the doublet X_n. Note that unlike the particle addition operator a_i of the general ASM theory, no topplings are assumed to take place on applying the t operators. However, we can express the toppling rules in terms of relaxation rules for the t operators. These turn out to be more convenient to work with than the toppling rules.

For the ASM on the doublet chain we can verify that the stable configuration corresponding to an unstable configuration can be determined by the following rules.

(i) A single toppling of source site would generate a waves by transferring particles outside the source doublet. The unstable doublets of type A and B generate waves in both sides by the following rules:

$$A^* \to t^{-1} A^* t\ , \qquad {}^*A \to t^{-1}\, {}^*A t\ ,$$
$$ {}^*B_1 \to t^{-1}\, {}^*B_1 t\ , \qquad B_2^* \to t^{-1} B_2^* t\ . \tag{3}$$

Here $X \to Y$ denotes that X relaxes to Y.

(ii) The relaxation of the configurations of type C generates waves only on one side and becomes stable,

$$ {}^*C_1 \to t^{-1} B_1\ , \quad C_2^* \to B_2 t\ . \tag{4}$$

The creation of waves stops when the starred configuration gets converted into the normal one.

(iii) Once generated, these operators t and t^{-1} are moved across the chain (t rightwards and t^{-1} leftwards) as follows: The operator t moves to the right of the doublets of type A and B_1, without changing them,

$$t A \to A t\ , \qquad t B_1 \to B_1 t\ . \tag{5}$$

Thus the operator t can be moved to the right of an arbitrary sequence of doublets A and B_1. This movement corresponds to a "wave of topplings" defined by Ivashkevich *et al.* [32].

(iv) When the wave of topplings traveling to the right hits a right stopper, it is stopped. We refer to the position of the stopper as the end point of the wave. After stopping the wave, the configurations of the right stopper and the doublet just left to the stopper change in the following way:

$$X t B_2 \to X' A\ , \quad X t C_2 \to X' B_2\ , \quad X t C_1 \to X C_2\ , \tag{6}$$

where $X = A, B_1, {}^*A, A^*, {}^*B, B^*, C^*$, and the corresponding X' are B_1, C_1, ${}^*B_1$, A, ${}^*C_1$, B_2, and C_2, respectively.

(v) At the right boundary one particle is dropped out of the system. Thus we have for the doublet configuration at the right boundary

$$A\, t \to B_1\ , \qquad B_1\, t \to C_1\ . \tag{7}$$

The corresponding rules for t^{-1} can be written down similarly.

To illustrate the use of these rules, we consider the following example. Let us take $L = 7$, and consider a recurrent configuration characterized by the string $AAAB_1C_1B_2A$. Add a particle at the site (3,2). The resulting configuration is $AAA^*B_1C_1B_2A$. The final configuration can be obtained by the repeated use of the rules given above,

$$\begin{array}{llllllll} & A & At^{-1} & A^*t & B_1 & C_1 & B_2 & A \quad \text{using (1),} \\ \to & At^{-1} & A & A^* & B_1 t & C_1 & B_2 & A \quad \text{using (3),} \\ \to t^{-1} & A & A & A^* & B_1 & C_2 & B_2 & A \quad \text{using (3)and(4),} \\ \to & B_2 & A & A^* & B_1 & C_2 & B_2 & A \quad \text{using (4)for } t^{-1}\ . \end{array} \tag{8}$$

Similarly after the second wave the configuration becomes

$$C_2AA^*C_1B_2B_2A\ , \tag{9}$$

after the third wave the configuration becomes

$$C_1AA^*C_2B_2B_2A\ , \tag{10}$$

and after the fourth wave the configuration becomes

$$B_1B_2AB_2B_2B_2A\ . \tag{11}$$

Now there is no unstable site so the avalanche stops. Clearly, working with the rules (1) to (5) is a quicker way to calculate the final configuration than brute force topplings. This method of transfer operator is easily generalized for other graphs. One will need more than one operator of this type $(t_1, t_2, \ldots)$ if there is more than one bond between the adjacent unit cells.

V. STRUCTURE OF THE AVALANCHES

In this section, we use the rules of propagation of particle transfer operator t described above to analyze the propagation of the avalanches. In the following, we shall refer to the site where the particle is added as the source of waves of topplings, or more simply, as the source site. Without loss of generality, we may assume that the source site is to the left of the BP.

Clearly, if the configuration of the doublet left of the source site is (3,2), the avalanche does not spread to the left, and propagates a distance of order L up to the BP on the right. Each site affected by the avalanche topples only once, and the total number of topplings in an avalanche is of order L. Such an avalanche is said to be of type I. It is easy to see that the probability that the addition of a particle will cause an avalanche of type I is $\frac{1}{4}$. The fraction of critical sites (sites, where addition of particle will cause an avalanche, in this case sites with height 3) is 3/4. Therefore, the fractional number of type I avalanches in all nontrivial avalanches (avalanches with at least one toppling) is 1/3. A picture showing the evolution of type I avalanche is shown in Fig. 2(a).

In all other conditions, the avalanche behaves qualitatively different from the type I avalanches. We call these type II avalanches. These avalanches travel a distance of $O(L)$ on both sides of the source point. In these avalanches, the motion of avalanche front is quite complicated as may be seen from Fig. 2(b) which shows the

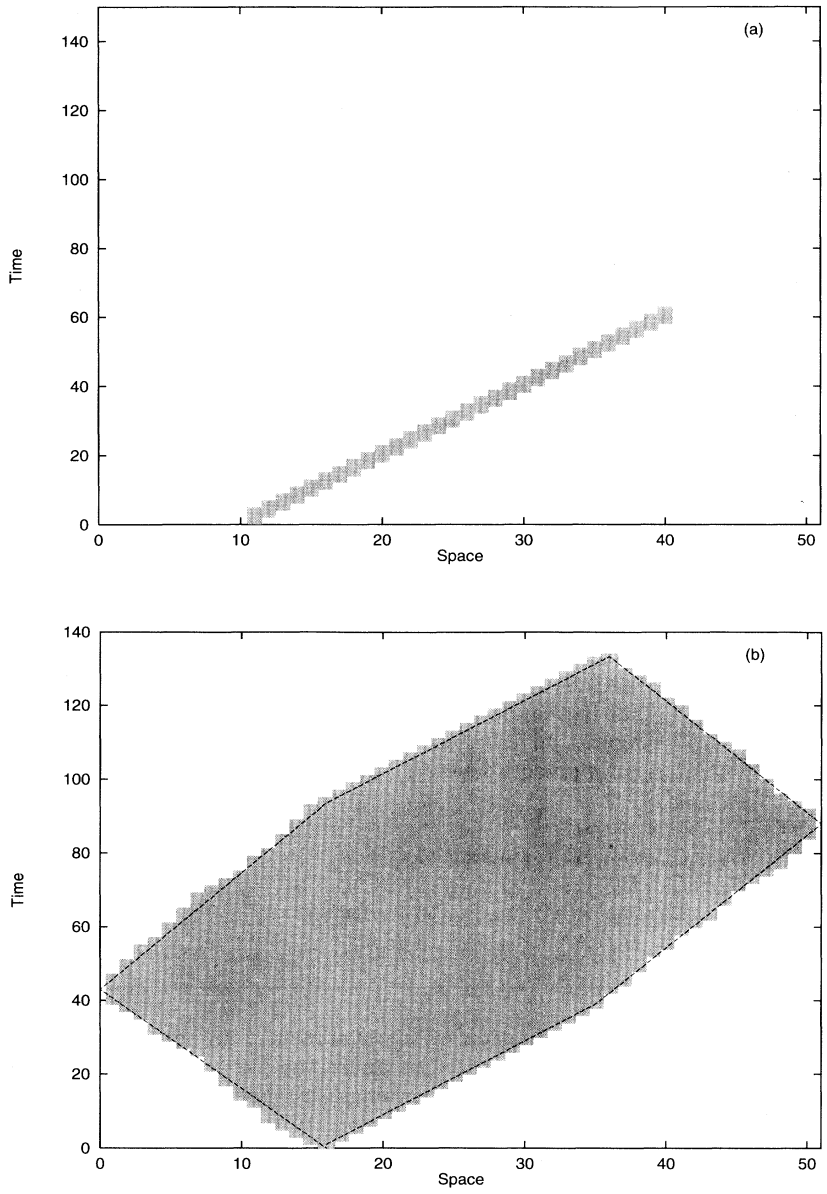

FIG. 2. The evolution of (a) type I avalanche, (b) type II avalanche in case A. The gray rectangles denote individual toppling events.

evolution of type II avalanche. The spread of avalanche is described in detail below.

The first right wave propagates to the BP. It crosses each doublet in two time steps. So the velocity of the avalanche front up to the BP is one doublet per two time step. The propagation of the avalanche front to the left is more complicated and shows an interesting stochastic structure. The first wave crosses all the A type doublets until it encounters the first doublet of type B_1. From rule (4), this B_1 type doublet stops the wave and becomes A type. The A type doublet just to the right of it becomes a B_2 type doublet. Neither of these two doublets is a left stopper. Therefore, the second wave crosses the end point of the first wave. It also crosses all the A type doublets coming after that, until it hits a B_1 type doublet. The doublet right to this doublet is again of type A. The changes in the doublet configurations occur in the same way as in the case of the first wave, and the next wave crosses the end point of the second wave. Note that the doublet just left of the end point of a wave is always of type A, and there are only B_2 or A types of doublets between the source point and the end point of the wave. Thus each wave crosses the end point of the previous wave and the avalanche keeps propagating leftward until it reaches the boundary. For a large time, the distance moved by the front increases linearly with time, and one can define an average linear velocity of the front.

The average velocity of the avalanche front in this case is easily calculated. Let the number of doublets of type B_1 between the source point and the left boundary be n. Then the avalanche takes n waves to reach the boundary. The waves start after alternate time steps, so the nth

wave starts after $2n$ time steps. It reaches the boundary in $2m$ time steps, where m is the number of doublets between the source point and the left boundary. Since the probability of occurrence of a B_1 type doublet is $1/2$ on the left of the break point, $n \sim m/2$. Thus the time taken by the avalanche to reach the boundary is $3m$. Therefore, the average velocity of the avalanche front is $1/3$ doublets per time step.

The $(n+1)$th wave reaches the boundary and drops a particle from the system. From the above discussion, we know that the doublet just right of the end point of a wave is always of type A. For this wave, it implies that the doublet at the boundary is of type A. After the completion of the wave it becomes of type B_2. The next wave also reaches the boundary and drops another particle. This converts the B_2 type doublet into a C_2 type doublet. The C_2 type doublet stops the next wave and the avalanche front starts receding. The subsequent waves make it C_1 and then B_1 [see rule (4)]. If the doublet just right of this A type doublet is of B_2 type, then it becomes C_2 type and stops the next wave. Otherwise, the next wave changes the B_1 type doublet into an A type doublet. Thus an A type doublet whose right neighbor is also of type A is changed in the following way by the subsequent waves:

$$A \rightarrow B_2 \rightarrow C_2 \rightarrow C_1 \rightarrow B_1 \rightarrow A \ . \tag{12}$$

If the right neighbor is of type B_1, then the above sequence terminates at B_1. The subsequence starting from B_2 explains the way the B_2 type doublet gets modified as the avalanche front recedes.

The number of waves required to change an A type doublet back to A type is five. Out of these waves the last two waves also change the configuration of the doublet just to the right. Thus the avalanche front takes three waves to cross an A type doublet. It takes two waves to cross a B_2 type doublet. Since the probability of B_2 type and A type doublets is equal, the avalanche takes $5m/2$ waves to recede. The time steps required to generate so many waves is $5m$. The wave that reaches the boundary takes $2m$ time steps more than the last wave, which terminates near the source point. Thus the time taken by the avalanche front to recede is $3m$. This shows that the effective backward velocity of the receding avalanche front is $1/3$ doublets per time steps.

If the distance between the BP and the source point is not sufficient, the avalanche may stop before reaching the boundary point on the left, as then the number of waves generated at the source point is less than n.

The propagation of the avalanche front after reaching the BP on the right of the source point is similar to that of the left front. Here doublets of type B_1 are the stoppers. We know that the first wave travels to the BP. If the BP is of type B_1 and the doublet just to the left is of type A, then the second wave crosses the BP. After this, each new right wave keeps moving further right until it reaches the right boundary. The probability that the configuration at BP is B_1 and the doublet to the left of it is A is $\frac{1}{6}$. In all other cases the next right wave does not cross the BP and the right avalanche front starts receding after having hit the BP. The forward and backward propagation of the right avalanche front after crossing the BP is exactly the same as that of the left avalanche front (with the role of B_1 and B_2 type doublets interchanged).

VI. PROBABILITY DISTRIBUTION OF AVALANCHE SIZES

For type I avalanches, the probability distributions of sizes of avalanches, as measured by the total number of topplings s, the total number of distinct sites toppled s_d, the duration t, and the number of times the source site topples n_c is calculated easily. It is convenient to work with the scaled variable $\alpha \equiv \frac{i}{L}$ and $\beta \equiv \frac{i'}{L}$, such that $\alpha,\ \beta \in [0,1]$, where i and i' are the position of source point and BP on the chain, respectively. Since, in these avalanches, one site topples at each time step

$$s = s_d = t = 2(\beta - \alpha)L \ , \tag{13}$$

and $n_c = 1$. Thus the probability distribution of s/L, s_d/L, and t/L for given α and β has a δ function at $2(\beta - \alpha)$. Averaging over α and β, we find for type I avalanches

$$\mathrm{Prob}_L(X, \text{ type I}) = \frac{1}{3}\left(1 - \frac{X}{2}\right) \quad \text{for} \quad 0 \le X \le 2 \ , \tag{14}$$

where $X = s/L,\ s_d/L,\ t/L$, and $1/3$ is the probability of occurrence of type I avalanche. In type I avalanches any site topples only once, so n_c is always 1.

Type II avalanches show a much complicated and interesting structure. In the preceding section, we have shown that the avalanche front does not move uniformly in time, and the spreading rate depends on the local height configuration. However, for distances much larger than 1, there is a nonzero average velocity. Thus at large length scales the space time history of the avalanche front is an approximate polygon (see Fig. 2). (The deviation from the polygonal shape is diffusive in character, which grows as $\sqrt{L}$, and can be neglected for large L.) The number of sides in the polygon depends on the position of the source point α and BP β and on whether the BP is crossed by the avalanche or not.

If the BP is not crossed by the avalanche, there are three distinct cases depending on the relative values of α and β. [Here we have assumed that $\alpha < \beta$. If $\alpha > \beta$, then the problem is the same as the mirror reflected problem with $\alpha \rightarrow (1-\alpha)$ and $\beta \rightarrow (1-\beta)$.]

(a) $0 < \alpha < 5\beta/11$, (b) $5\beta/11 < \alpha < 5\beta/6$, and (c) $5\beta/6 < \alpha < \beta$.

If the BP is crossed by the avalanche, there are four distinct cases:

(a) $0 < \alpha < \min((1-\beta)/6, \beta)$,
(b) $(1-\beta)/6 < \alpha < \min((6-\beta)/11, \beta)$,
(c) $(6-\beta)/11 < \alpha < \min((1-\beta/6), \beta)$,
(d) $(1-\beta/6) < \alpha < \beta$.

These are depicted in Figs. 3(a)–3(g).

The ranges of (α, β) corresponding to different cases

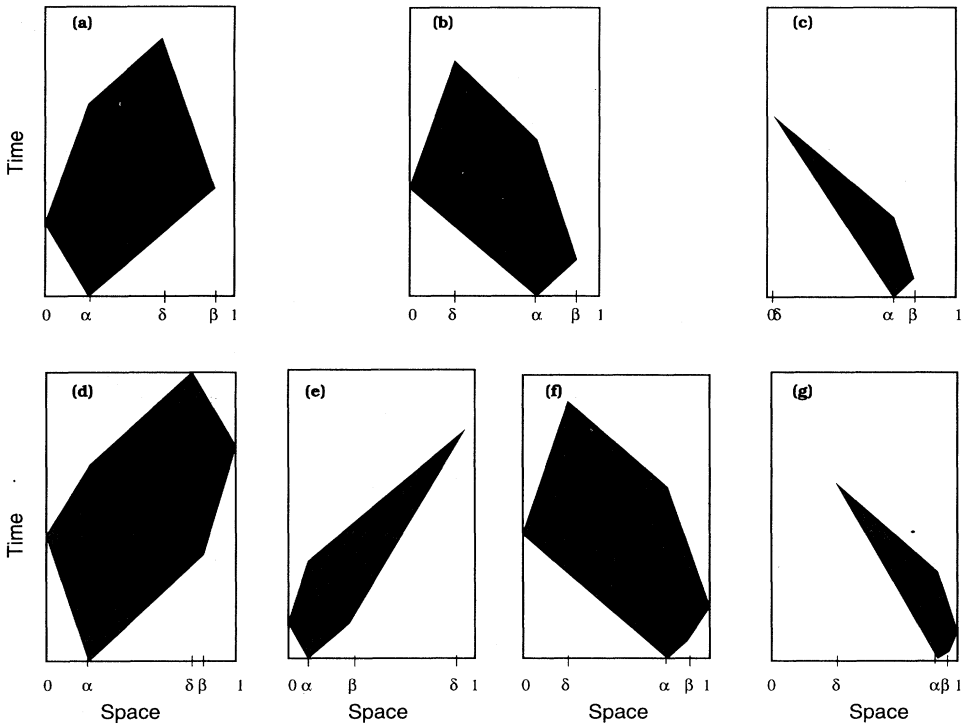

FIG. 3. Schematic diagram showing the evolution of various cases of type II avalanches. The scaled variables α, β, and δ denote the source point, the break point (BP), and the point where the last toppling occurs, respectively.

are easily determined from the known velocities of propagation of advancing and receding avalanche front.

Consider, for example, the case shown in Fig. 3(a). In this case the avalanche spreads to the BP on one side and reaches the boundary on the other side and δ, the point where the avalanche stops, is between α and β. To obtain δ we equate the time taken for the right and the left fronts to reach δ.

$$t/L = 3\alpha + 3\alpha + 2(\delta - \alpha) = 2(\beta - \alpha) + 3(\beta - \delta) \ . \quad (15)$$

This implies that

$$\delta = \beta - \frac{6}{5}\alpha \quad \text{and} \quad t = \frac{2}{5}(4\alpha + 5\beta)\, L \ . \quad (16)$$

The condition $\alpha < \delta < \beta$ immediately gives us the range $0 < \alpha < \frac{5}{11}\beta$.

In this case, clearly as all doublets left to the BP topple at least once,

$$s_d = 2\beta L \ . \quad (17)$$

The factor of 2 accounts for the number of sites in each doublet.

The number of topplings at the source site is half of the height of polygon at the source site, because the source site topples at alternate time steps. This gives

$$n_c = 3\alpha L \ . \quad (18)$$

The total number of toppling is equal to the area enclosed by the avalanche front. It can be easily calculated using simple geometry

$$s = \frac{3}{5}\alpha(10\beta - 11\alpha)\, L^2 \ . \quad (19)$$

Note that s_d, t, and n_c scale as L, because they are proportional to the linear size of the polygon, whereas s scales as L^2, because it varies as the area of the polygon. Therefore, for this type of avalanche it is convenient to use the following scaled variables:

$$\begin{aligned} S_d &\equiv s_d/L = 2\beta \ , \\ T &\equiv t/L = \tfrac{2}{5}(4\alpha + 5\beta) \ , \\ N_c &\equiv n_c/L = 3\beta \ , \\ S &\equiv s/L^2 = \tfrac{3}{5}\alpha(10\beta - 11\alpha) \ . \end{aligned} \quad (20)$$

Similar expressions for S_d, N_c, T, and S are easily written down in other cases. These are listed in the Appendix.

The probability distribution functions for given α and β are a sum of two δ functions corresponding to the cases whether the BP is crossed by the avalanche or not. Averaging over α and β we find

$$\text{Prob}_L\,(q, \text{ type II})$$

$$= \sum_{i=1,2} p_i \int_0^1 \int_0^1 d\alpha\, d\beta\, \delta(q - q_i(\alpha, \beta)) \ , \quad (21)$$

where $q = S, T, S_d, N_c$, and the subscripts 1 and 2 refer to the cases in which the BP is crossed, and those in which the BP is not crossed, respectively. The probability that the avalanche crosses the BP is $p_1 = 1/9$, and that it does not cross the BP is $p_2 = 8/9$.

Since S_d is the extension of the polygon along the horizontal axis, it is a linear function of α and β in each of

the seven cases. Hence the probability distribution of S_d is a piecewise linear function. The same argument works for T and N_c also. Explicitly, we find

$$\text{Prob}_L\ (S_d, \text{type II}) = \frac{5}{54}\left(1+\frac{21\,S_d}{10}\right)+\frac{5}{54}\delta\,(S_d-2)$$

$$\text{for}\quad 0<S_d<2\ ,$$

$$\text{Prob}_L\ (N_c, \text{type II}) = \frac{8}{27}(3-2\,N_c)$$

$$\text{for}\quad 0<N_c<\frac{3}{2}\ , \quad (22)$$

and

$$\text{Prob}_L\ (T, \text{type II})$$

$$=\begin{cases} \frac{2}{27}\left(1+\frac{16\,T}{9}\right) & \text{for}\ \ 0<T<2 \\ \frac{11}{27}\left(1-\frac{17\,T}{198}\right) & \text{for}\ \ 2<T<\frac{18}{7} \\ \frac{20}{27}\,(3-T) & \text{for}\ \ \frac{18}{7}<T<3\ . \end{cases} \quad (23)$$

The scaled variable S is proportional to the area of the polygon. Therefore, it is a quadratic function of α and β. However, this is a different quadratic function in different ranges of (α,β) corresponding to Figs. 3(a)–3(g). Substituting these formulas in Eq. (21) and doing the integration we get finally

$$\text{Prob}_L\ (S, \text{type II}) = -\frac{2}{9}+\sqrt{\frac{5}{243\,S}}+\frac{1}{27}\sqrt{\frac{5}{2}}\left[\arcsin\left(\frac{\sqrt{\frac{3}{11}}}{\sqrt{3-2\,S}}\right)-\arcsin\left(\frac{\sqrt{\frac{3}{11}}\,\left(-5+4\sqrt{3}\sqrt{3-7\,S}\right)}{7\sqrt{3-2\,S}}\right)\right]$$
$$+\frac{\ln(\frac{7}{5})}{54}-\frac{1}{27}\ln\left(\frac{\sqrt{\frac{3}{7}}\left(1-\sqrt{1-\frac{7\,S}{3}}\right)}{\sqrt{S}}\right)+\frac{5}{27}\ln\left(\frac{11\sqrt{S}}{\sqrt{15}\left(1-\sqrt{1-\frac{11\,S}{15}}\right)}\right)$$

$$\text{for}\ 0<S<\frac{5}{12}\ , \quad (24)$$

$$\text{Prob}_L\ (S, \text{type II}) = -\frac{1}{27}\sqrt{\frac{5}{2}}\left[\arcsin\left(\frac{\sqrt{\frac{3}{11}}\,\left(-5+4\sqrt{3}\sqrt{3-7\,S}\right)}{7\sqrt{3-2\,S}}\right)+\arcsin\left(\frac{\sqrt{\frac{3}{11}}\,\left(5+4\sqrt{3}\sqrt{3-7\,S}\right)}{7\sqrt{3-2\,S}}\right)\right]$$
$$\times\frac{1}{27}\left[\sqrt{10}\arcsin\left(\frac{\sqrt{\frac{3}{11}}}{\sqrt{3-2\,S}}\right)+5\ln\left(\frac{1+\sqrt{1-\frac{11\,S}{15}}}{1-\sqrt{1-\frac{11\,S}{15}}}\right)-2\ln\left(\frac{\sqrt{\frac{3}{7}},\left(1-\sqrt{1-\frac{7\,S}{3}}\right)}{\sqrt{S}}\right)\right]$$

$$\text{for}\ \frac{5}{12}<S<\frac{3}{7}\ , \quad (25)$$

$$\text{Prob}_L\ (S, \text{type II}) = \frac{1}{27}\sqrt{10}\arcsin\left(\frac{\sqrt{\frac{3}{11}}}{\sqrt{3-2\,S}}\right)+\frac{5}{27}\ln\left(\frac{1+\sqrt{1-\frac{11\,S}{15}}}{1-\sqrt{1-\frac{11\,S}{15}}}\right)\quad \text{for}\ \frac{3}{7}<S<\frac{15}{11}\ , \quad (26)$$

and

$$\text{Prob}_L\ (S, \text{type II}) = \frac{1}{27}\sqrt{\frac{5}{2}}\,\pi\quad \text{for}\ \frac{15}{11}<S<\frac{3}{2}\ . \quad (27)$$

Note that this probability distribution diverges for small S as $S^{-1/2}$ (see the second term in the first expression). The diverging contribution comes from case (d) of Fig. 3. In this case the linear size of the polygon is proportional to $\Delta\equiv(\beta-\alpha)$. Therefore, $S\sim\Delta^2$. As $\text{Prob}(\Delta)\sim$ const, for $\Delta\to 0$, we get the square-root singularity in the probability distribution of S for $S\to 0$.

Summing over the contribution coming from type I avalanches [Eq. (14)] and those of type II [Eq. (21)], we obtain the full probability distributions. Note that n_c and s scale differently for type I and type II avalanches, therefore the probability distributions of these quantities have the form given in Eq. (1). Other quantities such as s_d and t scale as L for both types of avalanches. Therefore, the distribution of these quantities has a simple scaling form.

In Fig. 4, we have plotted the probability distribution of s_d, t, n_c, s for type I avalanches, and s for type II avalanches. The diamonds denote the simulation results for the chain of size 100, and the solid line shows the theoretical expressions. The δ functions in the expression of s_d and n_c have not been shown. Note that our theoreti-

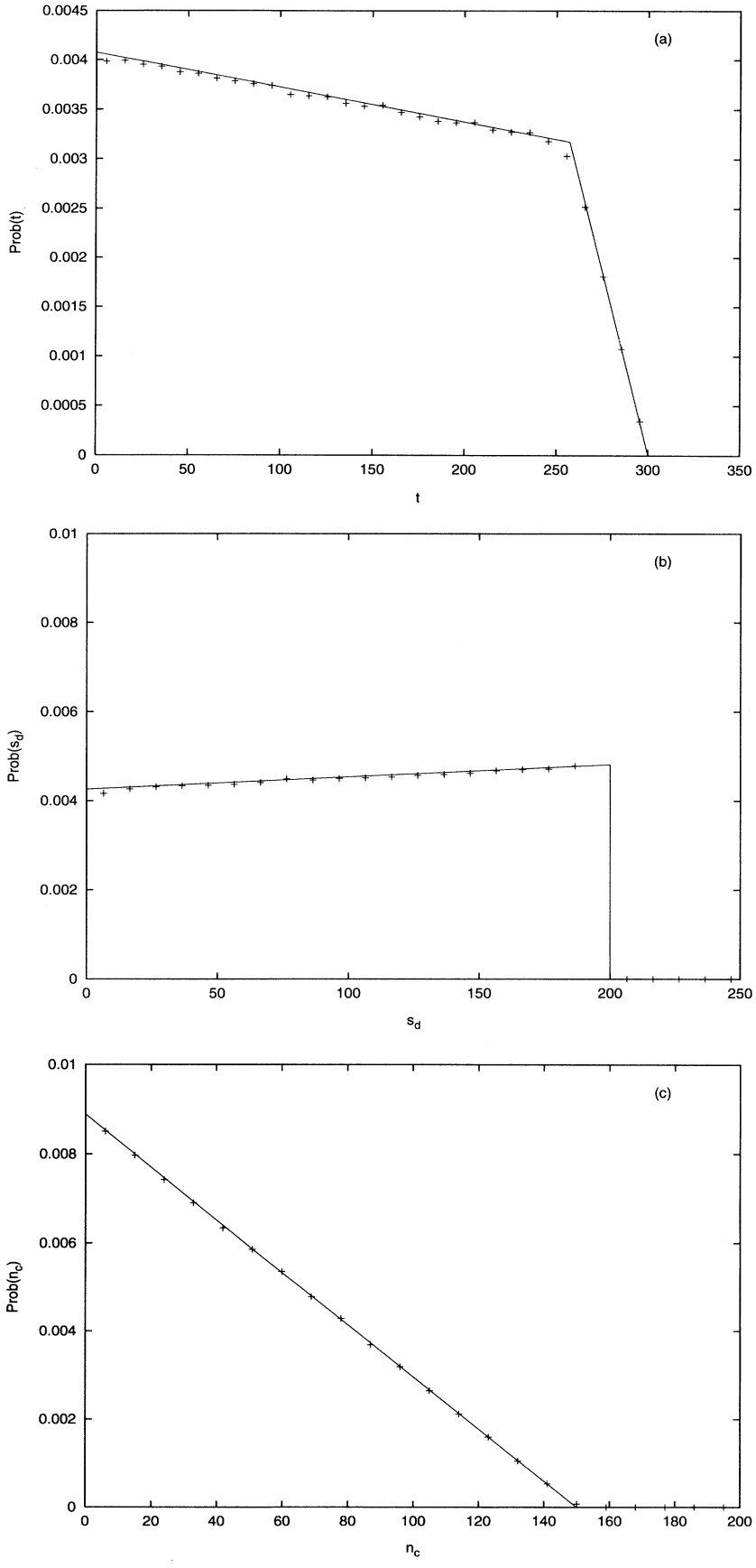

FIG. 4. The probability distributions of (a) t, (b) s_d, (c) n_c, (d) small s, and (e) large s. The numerical data in the small s regime agree with analytically obtained distribution of the linear avalanche and in the large s regime they agree with analytically obtained distribution of the compact avalanche. The numerical data are obtained from 500 000 avalanches on a lattice of size 250.

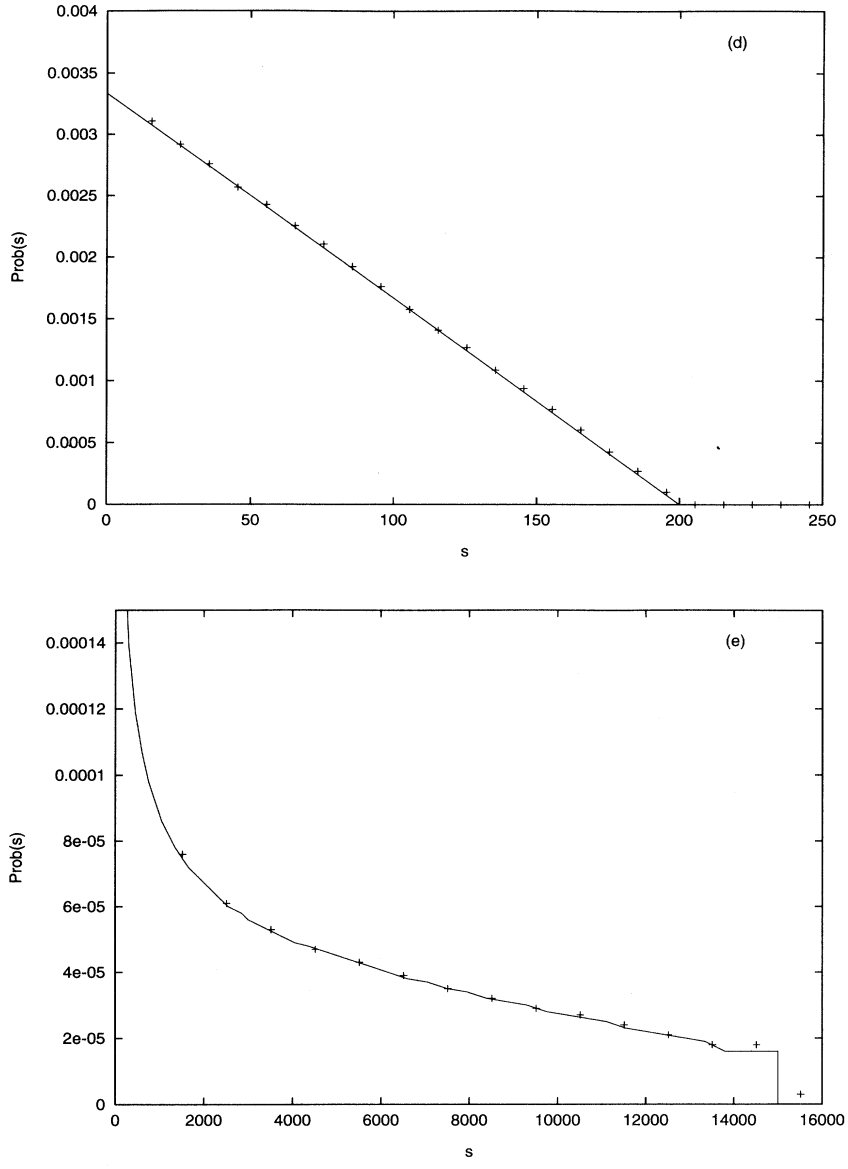

FIG. 4 *(Continued).*

cal results show excellent agreement with the numerical results even for L as small as 100.

VII. MULTIFRACTALITY IN PROBABILITY DISTRIBUTION OF AVALANCHE SIZES

In the multifractal description one defines the function $f(\alpha)$ by the condition that the probability distribution of avalanches of size $X \sim L^{\alpha}$ scales as $L^{f(\alpha)}$, for large L. The explicit form of $f(\alpha)$ is given by

$$f(\alpha) = \lim_{L\to\infty} \ln[\mathrm{Prob}_L(X = L^{\alpha})]/\ln(L) \ . \qquad (28)$$

Thus the exponent $f(\alpha)$ is a function of the α. For our Abelian model it is easy to see from Eq. (1) that $f(\alpha)$ for $X = s$ is a nonincreasing piecewise linear function given by

$$f(\alpha) = \begin{cases} -1 - \frac{1}{2}\alpha & \text{for } 1 \le \alpha \le 2 \\ -1 & \text{for } 0 \le \alpha \le 1 \ . \end{cases} \qquad (29)$$

In Fig. 5, we have shown results of a computer simulation of the model for $L = 100$ for 2×10^5 avalanches. Also shown is the theoretical curve using Eq. (1) for $L = 100$ (dotted line) and $L = \infty$ (solid line). Clearly, there is a very good agreement with simulation data. We note that the f versus α curve is quite similar (nonincreasing piecewise linear) to that obtained in [20]. Also note that the approach to the $L \to \infty$ limit is quite slow, because the corrections decrease as only $1/\ln(L)$.

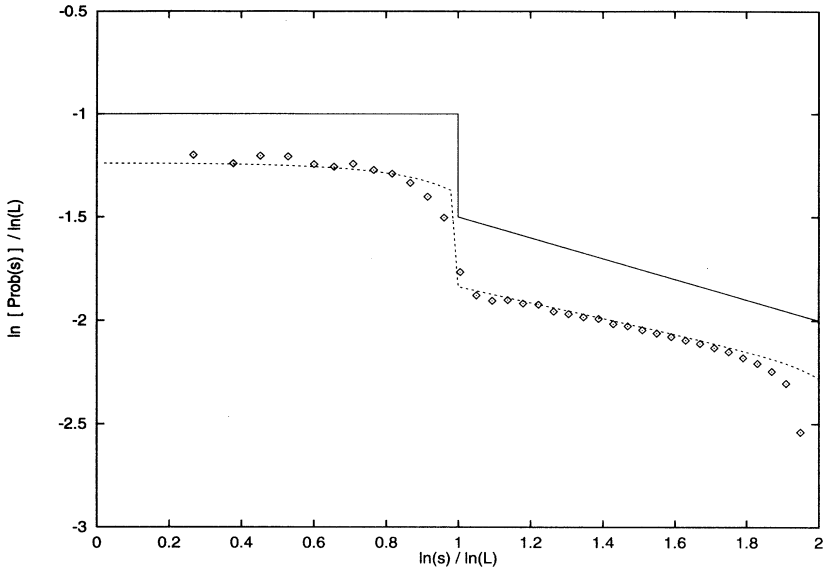

FIG. 5. The log-log plot of Prob(s) vs s. The solid line shows the exact asymptotic behavior for $L \to \infty$, and the dotted line shows the theoretical curve for $L = 100$.

VIII. OTHER DECORATED CHAINS

In principle, the treatment may be extended to other types of unit cells also. However, the analysis is considerably more difficult even for slightly more complicated unit cells. We omit the details and only summarize the results for case B, where the unit cell is a diamond. In this case the number of allowed configurations of the diamond on both sides of the BP is four. As a result, the entropy per unit site is $\ln(4)/4$. In this case also, the avalanches spread at least up to the BP on one side of the source point and to a distance either of order L or of order 1 on the other side. Thus again, there are two types of avalanches which have the same scaling properties as the type I and type II avalanches of case A. A detailed calculation shows that these occur with relative frequencies 5:8 on the average.

The propagation of avalanche front in this case is more complicated than case A. In Fig. 6, we show a typical type II avalanche. We see that the avalanche front has an erratic, zigzag motion, which goes forward and backward many times depending on the local diamond height configuration. However, the time taken by the front to travel a long distance r is proportional to r [up to $O(\sqrt{r})$ corrections]. Thus, one can define asymptotic velocities of fronts. The outward velocity up to the BP is 1/3 diamonds per time step. The average outward velocity beyond the BP and also on the other side of the source point is 1/6 diamonds per time step. The average velocity of receding avalanche front is 1/10 diamonds per time step.

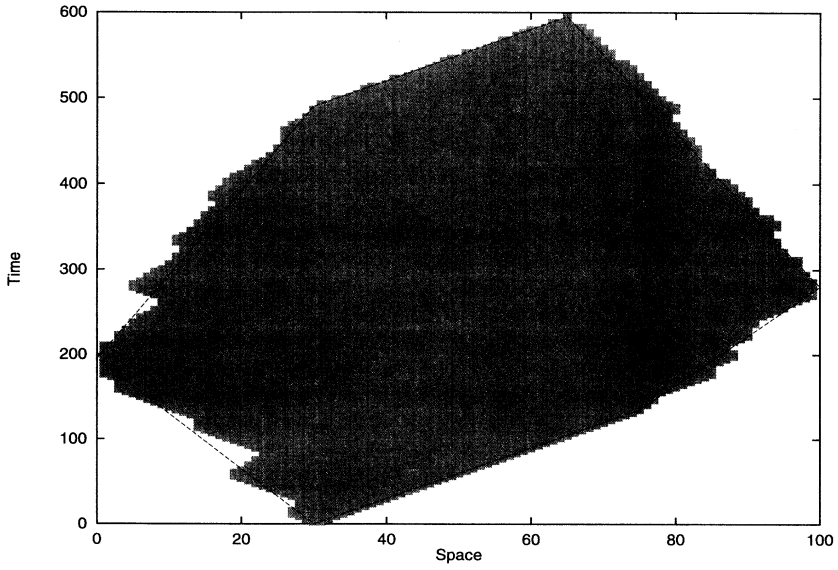

FIG. 6. The evolution of a type II avalanche in case B.

The analysis of the preceding section can be repeated *in toto* beyond this point. The probability distribution functions for both type I and type II avalanches have the same qualitative features irrespective of the velocities. For type I avalanches, $t \sim s_d \sim (\beta - \alpha)L$ to order L. Thus the probability distribution of s_d and t have the same linear form as in case A, while the slope depends on the velocities. The variable n_c has the probability distribution $\text{Prob}(n_c) \sim 2^{-n_c}$. As $s \sim n_c(\beta-\alpha)L$, this implies that the scaling function f_1 in Eq. (1) is a piecewise linear function with infinitely many segments.

For type II avalanches the space time history of active sites forms a polygon. The slopes of edges of the polygon depend on the velocities. As a result, the probability distributions have the same qualitative behavior as in case A. The exact form of functions f_1 and f_2 are not the same in cases A and B, and this proves that these functions are *not universal.* In case C, there are no avalanches of type I, and the simple scaling ansatz works [25].

IX. SUMMARY AND DISCUSSION

To summarize, we have studied the Abelian sandpile model on one-dimensional decorated chains. The calculation of structure of avalanche can be simplified by using the particle transfer operator, which was motivated by the technique of decomposition of avalanche into the waves of topplings introduced by Ivashkevich *et al.* We determined an exact asymptotic finite-size scaling behavior of the distribution of avalanche sizes. We find that the behavior of ASM on these chains is very different from that on the simple linear chain. The number of recurrent configurations in the steady state grows exponentially with the size of the chain and the critical state is not translationally invariant. There are two types of avalanches, type I and type II, which show different scaling properties. As a result, the probability distribution of the total number of topplings s and the number of times the site of addition of particles toppled n_c in an avalanche can be described by a linear combination of two simple scaling forms (LC2SSF), but not by the simple scaling form. We find that this scaling form is quite robust, and holds for several different one-dimensional conservative Abelian sandpile models.

As the LC2SSF involves only a finite number of unknown parameters, its use when simple scaling fails is preferable over the more general multifractal form (which corresponds to a linear combination of infinitely many simple scaling forms). We also note that we find the breakdown of simple scaling without the appearance of new length scales in our model.

Similar behavior may be expected in other one-dimensional models. For example, consider the ASM on an $L \times M$ cylinder with open boundary condition at the ends. For $L \gg M$, this lattice is effectively one dimensional. We expect three types of avalanches: type I and II, and finite avalanches of size $< M$, which do not ring the cylinder, and are two dimensional in character. This suggests that a LC3SSF would describe this situation. It remains to be seen whether this behavior survives in higher dimensions or if it is specific to one-dimensional models.

APPENDIX

In this appendix we list the expression of T, S_d, N_c, and S for various cases shown in Fig. 3. Case (a) has been dealt with in the text. Here we consider cases (b)–(h).

Case (b). In this case δ is between 0 and α. Hence δ is given by

$$\delta = \frac{1}{5}(5\beta - 6\alpha) \tag{A1}$$

and

$$\begin{aligned} T &= \tfrac{3}{5}(5\beta - \alpha)\ , & S_d &= 2\beta\ , \\ N_c &= \tfrac{5}{2}(\beta - \alpha)\ , & S &= \tfrac{3}{5}\alpha(10\beta - 11\alpha). \end{aligned} \tag{A2}$$

Case (c). For this case $\delta = 6\alpha - 5\beta$ and

$$\begin{aligned} T &= 15(\beta - \alpha)\ , & S_d &= 12(\beta - \alpha)\ , \\ N_c &= \tfrac{5}{2}(\beta - \alpha)\ , & S &= 15(\beta - \alpha)^2\ . \end{aligned} \tag{A3}$$

Case (d). For this case $\delta = \frac{1}{5}(6 - 6\alpha - \beta)$ and

$$\begin{aligned} &T = \tfrac{2}{5}(6 + 4\alpha - \beta)\ , \quad S_d = 2, \\ &N_c = 3\alpha\ , \\ &S = \tfrac{3}{5}(-1 + 12\alpha + 2\beta - 2\alpha\beta - 11\alpha^2 - \beta^2). \end{aligned} \tag{A4}$$

Case (e). For this case $\delta = 6\alpha + \beta$ and

$$\begin{aligned} T &= 16\alpha + 2\beta\ , & S_d &= 12\alpha + 2\beta\ , \\ N_c &= 3\alpha\ , & S &= 3\alpha(5\alpha + 2\beta)\ . \end{aligned} \tag{A5}$$

Case (f). For this case $\delta = \frac{1}{5}(6 - 6\alpha - \beta)$ and

$$\begin{aligned} &T = \tfrac{3}{5}(6 - \alpha - \beta)\ , \quad S_d = 2\ , \\ &N_c = \tfrac{1}{2}(6 - \beta - 5\alpha)\ , \\ &S = \tfrac{3}{5}(-1 + 12\alpha + 2\beta - 2\alpha\beta - 11\alpha^2 - \beta^2)\ . \end{aligned} \tag{A6}$$

Case (g). For this case $\delta = 6\alpha + \beta - 6$ and

$$\begin{aligned} T &= 3(6 - 5\alpha - \beta)\ , & S_d &= 2(7 - 6\alpha - \beta)\ , \\ N_c &= \tfrac{1}{2}(6 - \beta - 5\alpha)\ , & S &= 3(1 - \alpha)(7 - 2\beta - 5\alpha)\ . \end{aligned} \tag{A7}$$

[1] P. Bak, C. Tang, and K. Wiesenfeld, Phys. Rev. Lett. **59**, 381 (1987).
[2] A. Mehta and G. C. Barker, Europhys. Lett. **27**, 501 (1994).
[3] C. P. C. Prado and Z. Olami, Phys. Rev. A **45**, 665 (1992).
[4] R. E. Snyder and R. C. Ball, Phys. Rev. E **49**, 104 (1994).
[5] L. P. Kadanoff, S. R. Nagel, L. Wu, and S. M. Zhou,

Phys. Rev. A **39**, 6524 (1989).
[6] S. S. Manna, Physica A **179**, 249 (1991).
[7] K. Chen, P. Bak, and S. P. Obukhov, Phys. Rev. A **43**, 625 (1990).
[8] A. Sornette and D. Sornette, Europhys. Lett. **9**, 197 (1989).
[9] B. Drossel and F. Schwabl, Phys. Rev. Lett. **69**, 1629 (1992).
[10] E. N. Miranda and H. J. Herrmann, Physica A **175**, 339 (1991).
[11] M. Sasai, I. Ohime, and R. Ramaswamy J. Chem. Phys. **96**, 3045 (1992).
[12] Z. Olami, H. J. S. Feder, and K. Christensen, Phys. Rev. Lett. **68**, 1244 (1992).
[13] A. A. Middleton and C. Tang, Phys. Rev. Lett. **74**, 742 (1995).
[14] A. A. Ali (unpublished).
[15] T. Hwa and M. Kardar, Phys. Rev. Lett. **62**, 1813 (1989).
[16] G. Grinstein, D. H. Lee, and S. Sachdev, Phys. Rev. Lett. **64**, 1927 (1990).
[17] D. Dhar, Phys. Rev. Lett. **64**, 1613 (1990).
[18] J. Krug, J. Stat. Phys. **66**, 1635 (1992).
[19] S. C. Lee, N. Y. Liang, and W. J. Tzeng, Phys. Rev. Lett. **67**, 1479 (1991).
[20] A. B. Chhabra, M. J. Feigenbaum, L. P. Kadanoff, A. J. Kolan, and I. Procaccia, Phys. Rev. E **47**, 3099 (1993).
[21] S. N. Majumdar and D. Dhar, J. Phys. A **24**, L357 (1991).
[22] S. N. Majumdar and D. Dhar, Physica A **185**, 129 (1992).
[23] V. B. Priezzhev, J. Stat. Phys. **74**, 955 (1994).
[24] V. B. Priezzhev, D. V. Ktitarev, and E. V. Ivashkevich (unpublished).
[25] P. Ruelle and S. Sen, J. Phys. A **25**, L1257 (1992).
[26] D. Dhar and S. N. Majumdar, J. Phys. A **23**, 4333 (1990).
[27] S. A. Janowski and C. A. Laberge, J. Phys. A **26**, L973 (1993).
[28] D. Dhar and R. Ramaswamy, Phys. Rev. Lett. **63**, 1659 (1989).
[29] D. Dhar, P. Ruelle, S. Sen, and D. N. Verma, J. Phys. A **28**, 805 (1995).
[30] A. A. Ali and D. Dhar, Phys. Rev. E **51**, R2705 (1995).
[31] P. Bak, C. Tang, and K. Wiesenfeld, Phys. Rev. A **38**, 364 (1988).
[32] E. V. Ivashkevich, D. V. Ktitarev, and V. B. Priezzhev, Physica A **209**, 347 (1994).
[33] E. R. Speer, J. Stat. Phys. **71**, 61 (1993).
[34] D. Dhar and S. S. Manna, Phys. Rev. E **49**, 2684 (1994).

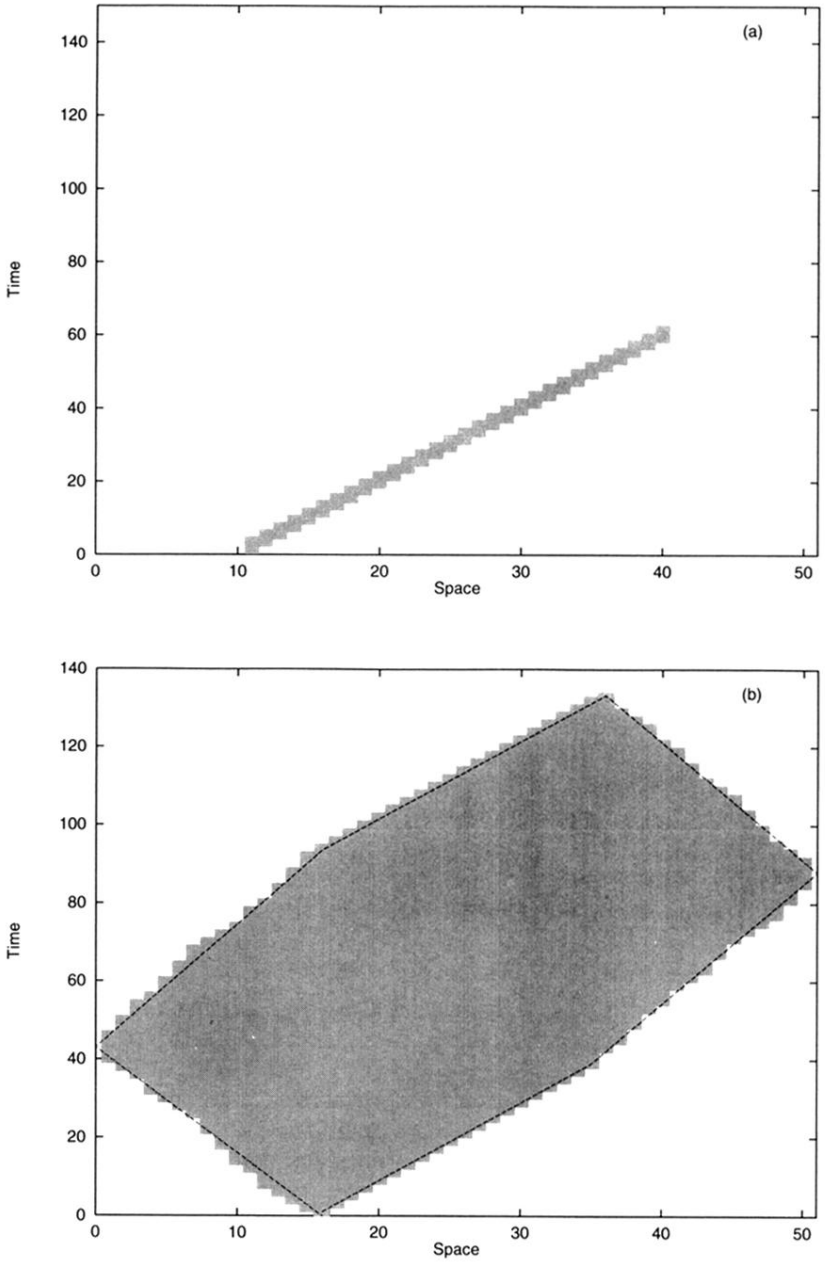

FIG. 2. The evolution of (a) type I avalanche, (b) type II avalanche in case A. The gray rectangles denote individual toppling events.

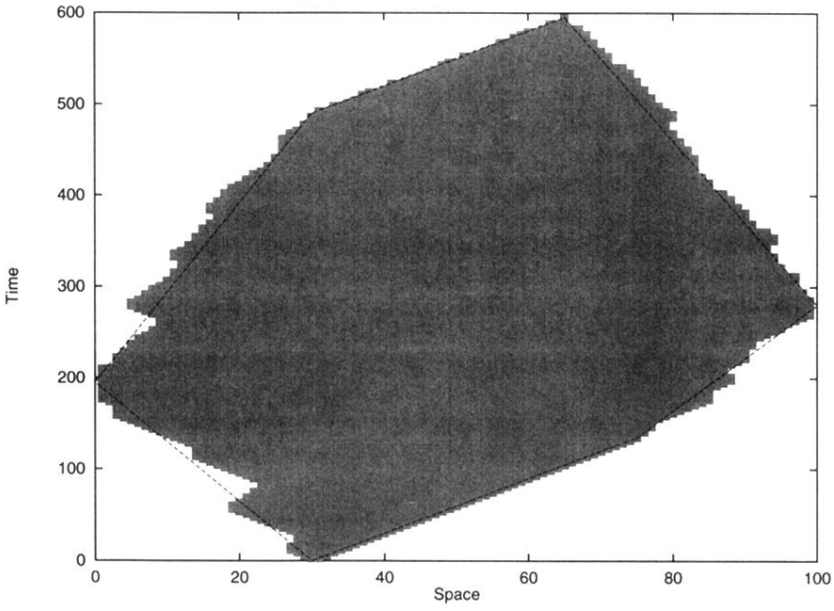

FIG. 6. The evolution of a type II avalanche in case B.